

# Chinese stalagmite $\delta^{18}\text{O}$ controlled by changes in the Indian monsoon during a simulated Heinrich event

Francesco S. R. Pausata<sup>1,2\*</sup>†, David S. Battisti<sup>2,3</sup>, Kerim H. Nisancioglu<sup>1,4</sup> and Cecilia M. Bitz<sup>3</sup>

**Carbonate cave deposits have been used to reconstruct the intensity of monsoon precipitation in areas influenced by the East Asian and Indian monsoon systems, because the  $\delta^{18}\text{O}$  of the carbonate tracks the isotopic signature of precipitation. These records indicate that monsoon strength was altered during the millennial-scale climate variations known as Dansgaard-Oeschger events and during the more prolonged Heinrich cooling events. Here we use a numerical climate model with an embedded oxygen-isotope model to assess what caused the shifts in the oxygen-isotope signature of precipitation during a climate perturbation designed to mimic a Heinrich event. Our simulations show that the cooling of the Northern Hemisphere—particularly the surface of the Indian Ocean—during the event reduces precipitation over the Indian basin and weakens the Indian monsoon. This leads to the export of water vapour enriched in the  $^{18}\text{O}$  isotope from India to China. Our model broadly reproduces the enrichment of  $\delta^{18}\text{O}$  over East Asia evident in speleothem records during Heinrich events. We therefore conclude that changes in the  $\delta^{18}\text{O}$  of cave carbonates over millennial and precessional timescales reflect changes in the intensity of Indian rather than East Asian monsoon precipitation.**

**D**uring the last glacial period (~110–10 kyrs BP), millennial-scale climate variability was characterized by abrupt transitions between cold stadial and warm interstadial states. Several of these cold stadial periods are interrupted by extreme ice-rafting events, the so-called Heinrich events (H-events)<sup>1</sup>. H-events, as well as the more recent Younger Dryas (YD, sometimes referred to as H0), are large freshwater discharges from the North American ice sheet into the North Atlantic occurring irregularly throughout the ice age, causing long-lived cold states<sup>2</sup>; seven H-like events occurred during the last glacial period<sup>3</sup>. The climate changes coincident with H-events are not restricted to the North Atlantic basin, but are communicated over large parts of the globe<sup>4,5</sup> through changes in atmospheric and ocean circulation in response to rapid changes in Nordic Sea sea-ice extent<sup>6–8</sup>.

The rapid climate changes associated with the most recent H-event (H1) and the YD are faithfully recorded in the oxygen-isotopic composition of stalagmites (speleothems) throughout South and East Asia (see, for example, refs 9–12). The oxygen-isotopic composition of the stalagmite calcite ( $\delta^{18}\text{O}_c$ ) reflects the temperature of the cave and the precipitation-weighted  $\delta^{18}\text{O}$  of precipitation ( $\delta^{18}\text{O}_p$ ; see Methods) at the cave site. A change in  $\delta^{18}\text{O}_p$  may result from a change in several local and non-local processes, including: the ratio of summer-to-spring precipitation (seasonality of precipitation affects  $\delta^{18}\text{O}_p$  because summer rainfall has lighter (more negative)  $\delta^{18}\text{O}$  values compared with spring precipitation<sup>13–15</sup>); the intensity of precipitation falling at a given location (amount effect<sup>16</sup>) owing to changes in the strength of the convection; the origin of the water vapour delivered to the site owing to changes in circulation; the isotopic composition (not the amount) of water vapour that is arriving from one or more regions owing to changes in the processing of water vapour

en route from the source and the isotopic composition of the source (for example, owing to changes in sea surface temperature (SST) or river runoff<sup>17</sup>).

Oxygen-isotope records in speleothems throughout Asia are often interpreted as an index for the ‘strength’ or ‘intensity’ of Asian monsoons, because they feature large oscillations in  $\delta^{18}\text{O}_c$  that are highly correlated with changes in local summer insolation due to the precession of the equinoxes (see, for example, refs 11,13). Several studies have suggested that orbital variations cause changes in  $\delta^{18}\text{O}_c$  by changing local precipitation processes and/or amounts<sup>13,15,18,19</sup>, including, for example, variations in the seasonality of precipitation. Recent studies, however, suggest that it is difficult to explain the influence of orbital variations on isotopes in the Asian cave records through local climate changes (for example refs 20,21) and that the cave records more probably reflect changes in the  $\delta^{18}\text{O}$  of water vapour due to non-local climate processes, including changes in the processing of the vapour en route to the caves and changes in the fractionation at the source (land or ocean)<sup>20–23</sup>.

The millennial-scale variations in  $\delta^{18}\text{O}_c$  captured in cave records throughout southern and eastern Asia and associated with abrupt climate changes, such as H-events, are about one-third of the amplitude of the precessional changes<sup>13</sup>. This is remarkable because it indicates that variability in the ‘monsoon strength’ on millennial timescales, which is due to dynamics internal to the Earth’s climate system, is of the same order as that associated with the orbitally forced changes. In this study, we shall use models to examine the changes in climate and in the isotopic composition of precipitation that result from a sudden change in sea-ice extent in the northern North Atlantic, which is thought to be the causal agent of global climate changes associated with H-events. Our particular goal is to understand the

<sup>1</sup>Bjerknes Center for Climate Research, Bergen, Norway, <sup>2</sup>Geophysical Institute, University of Bergen, Bergen, Norway, <sup>3</sup>Department of Atmospheric Sciences, University of Washington, Seattle, Washington, USA, <sup>4</sup>UNI Research, Bergen, Norway. <sup>†</sup>Present address: Joint Research Center, Institute for Environment and Sustainability, Ispra (VA), Italy. \*e-mail: francesco.pausata@jrc.ec.europa.eu.

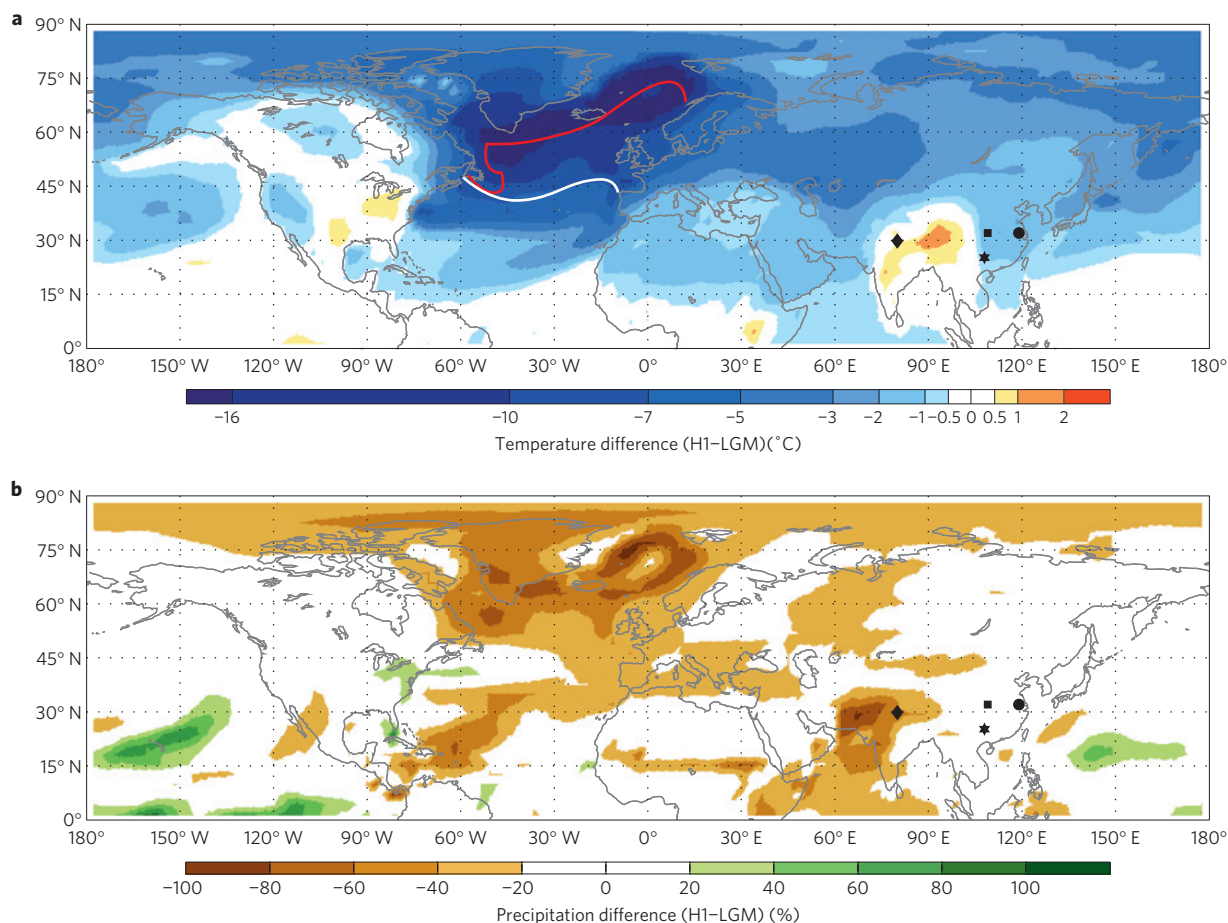


**Figure 1 | Annual averaged temperature and precipitation between the H1 and LGM. a**, Surface temperature difference (°C). **b**, Precipitation difference (%). Markers indicate the locations of the following caves: Hulu (circle), Songjia (square), Dongge (star) and Timta (diamond). The lines in **a** indicate the annual climatological 50% sea-ice extent for H1 (white) and LGM (red) in the North Atlantic sector.

1 climatological significance of the signals recorded in the  $\delta^{18}\text{O}_c$  of  
2 Asian speleothems.

### 3 Simulated isotopic change due to an archetypal H-event

4 We take as a starting point the climate of the Last Glacial  
5 Maximum (LGM) as simulated by a fully coupled climate  
6 model (Community Climate System Model version 3, CCSM3) using  
7 insolation, carbon dioxide, ice sheets and continental geometry  
8 from 21 kyrs BP (ref. 24). A second set of experiments (H1)  
9 was carried out in which freshwater is abruptly added to the  
10 North Atlantic to mimic an H-event (see Methods), causing an  
11 extensive expansion of sea ice in the northern North Atlantic<sup>25</sup>.  
12 We call these experiments ‘H1’ because they feature an extension  
13 of sea ice in the North Atlantic that is consistent with the  
14 extension of ice-covered area in a typical H-event<sup>1</sup> and because  
15 the sedimentary chronology is unambiguously tied to the cave  
16 chronologies for the H1 event<sup>26</sup>. The coupled climate model used  
17 in the LGM and H1 experiments does not contain an isotope  
18 module. Hence, to examine the isotopic changes associated with  
19 the sudden expansion of sea ice in the North Atlantic, we ran two  
20 further off-line experiments using the same atmospheric model  
21 (Community Atmosphere Model version 3, CAM3; ref. 27) as is  
22 used in CCSM3, but with an embedded module for stable water  
23 isotopes<sup>28</sup>. These experiments use the same (21 kyr BP) boundary  
24 conditions as the coupled experiments. The annual cycle in SST  
25 and sea-ice concentration is prescribed to be identical to that from  
26 the coupled LGM experiment and from the ensemble average of  
27 the H1 experiments.

The difference in climate between the H1 and LGM simulations  
(Fig. 1) is due to the decrease in SST and especially the expansion  
of sea ice over the northern North Atlantic, causing a strong cooling  
extending throughout the Northern Hemisphere, as also shown in  
previous studies (for example refs 5,7,29; the simulated warming  
over northeast India is discussed in Supplementary Information).  
Precipitation is greatly reduced throughout the North Atlantic  
and northern Indian Ocean in the H1 experiment. Note that  
there are no significant changes in the annual average or seasonal  
distribution of precipitation at the location of the Chinese caves  
(Fig. 1, Table 1). The atmospheric circulation and the spatial and  
seasonal changes in surface temperature and precipitation in the  
uncoupled experiments are very similar to those from the coupled  
experiments (compare Fig. 1 and Supplementary Fig. S1). This  
enables us to use the uncoupled LGM and H1 experiments to  
determine changes in the isotopic composition of precipitation  
associated with abrupt changes in the North Atlantic sea ice.

The simulated change (H1 minus LGM) in  $\delta^{18}\text{O}_p$  over south  
Asia is shown in Fig. 2. The increase in  $\delta^{18}\text{O}_p$  in southern  
and eastern Asia is primarily due to changes in the  $\delta^{18}\text{O}$  and  
amount of precipitation during the monsoon season—May to  
August (MJA; Supplementary Fig. S2). The cooler H1 climate  
features an increase in  $\delta^{18}\text{O}_p$  throughout southern and eastern  
Asia, including all cave sites, ranging from +0.9‰ at Hulu to  
+1.7‰ at Timta. Taking into account the temperature-dependent  
fractionation<sup>30</sup> of calcite and the change in temperature simulated  
for H1, the  $\delta^{18}\text{O}$  change that would have been recorded in the  
stalagmites in Hulu and Timta caves ( $\Delta\delta^{18}\text{O}_c$ ) would be +1.3‰ and

**Table 1 | Impact of an abrupt cooling event on the climate and isotopic composition of precipitation at the four cave sites.**

Cave	Change in annual		JJA/MAM precip.		Change in		Contribution of	
	temp. (°C)	precip. (%)	LGM	H1	obs. $\delta^{18}\text{O}_c$	sim. $\delta^{18}\text{O}_p$ ( $\delta^{18}\text{O}_c$ )	precip.	$\delta^{18}\text{O}$
Hulu, China	-1.9	-4	0.99	0.92	+1.4	+0.9 (+1.3)	+0.2	+0.9
Songjia, China	-1.9	0	1.47	1.52	+1.4	+1.1 (+1.5)	+0.1	+1.2
Dongge, China	-0.9	-9	1.32	1.33	+1.0	+1.0 (+1.2)	+0.1	+1.1
Timta, India	+0.4	-47	6.67	2.78	+3.0	+1.7 (+1.7)	+0.8	+3.2

From left to right: change in annually averaged surface temperature (°C) and precipitation amount (%); ratio of summer (JJA) to spring (MAM) precipitation at the cave locations; change in the observed  $\delta^{18}\text{O}$  of calcite ( $\delta^{18}\text{O}_c$  VPDB, in ‰; refs 9–12) and change in modelled  $\delta^{18}\text{O}_p$  Vienna Standard Mean Ocean Water (in parentheses, change in modelled  $\delta^{18}\text{O}_c$  VPDB). The last two columns indicate modelled changes in the  $\delta^{18}\text{O}_p$  due to changes in the amount of precipitation only (that is, with no changes in the  $\delta^{18}\text{O}$  of precipitation) and due to changes in the  $\delta^{18}\text{O}$  of precipitation only (that is, with no changes in the amount of precipitation). See also Methods.

1.7‰ ( $\Delta\delta^{18}\text{O}_c = \Delta\delta^{18}\text{O}_p - 0.24\text{‰} \times \Delta T$ ), respectively, where  $\Delta T$  is the temperature change (Fig. 1 and Table 1). These results are in fair agreement with the observed increase in  $\delta^{18}\text{O}_c$  at the cave sites associated with an H-event or the onset of the YD (Table 1 and Fig. 2; see also Methods).

### Causes of $\delta^{18}\text{O}_p$ changes in Asian speleothems

At Timta and throughout northern India, the increase in  $\delta^{18}\text{O}_p$  is due to a ~50% reduction in summer precipitation (seasonality) and to an increase in the  $\delta^{18}\text{O}$  of the precipitation that is falling due to non-local changes (Table 1; Fig. 2 and Supplementary S3). In contrast, the increase in  $\delta^{18}\text{O}_p$  throughout eastern Asia, including at the locations of the Chinese caves, is almost entirely due to non-local changes in the  $\delta^{18}\text{O}$  of the precipitation, because neither the total amount nor the seasonality of precipitation has changed (Table 1, Supplementary Fig. S2). The three non-local processes that can affect the isotopic composition of precipitation in the model are (1) a change in the origin of the water vapour that is delivered (changes in circulation), (2) a change in the fractionation of oxygen isotopes in the water vapour en route to the cave site and/or (3) a change in the fractionation of oxygen isotopes at the source (for example, due to changes in the SST). To evaluate the first possibility we tag the water vapour from ten selected regions (four in the Tropical Pacific, two in the Indian Ocean, the North and South Pacific Ocean, the continents, and everywhere else; Supplementary Fig. S4) and follow it until it precipitates. At every point on the globe and every point in time, we record the amount, isotopic composition and origin of the vapour that precipitates. Comparing the H1 and LGM experiments, we find that there are no changes of consequence in the mix of source regions that gives the net precipitation over southern and eastern Asia (Supplementary Fig. S5).

The second non-local process affecting the  $\delta^{18}\text{O}$  of precipitation (hence,  $\delta^{18}\text{O}_p$ ) is a change in the processing of water vapour en route from the source to the site where the vapour is precipitated. For example, a decrease in the amount of precipitation along the path between the source and the recording site leads to heavier  $\delta^{18}\text{O}$  of precipitation at the site because there is less rain-out of moisture during transport and therefore less fractionation. Our results show that a cooler Indian Ocean in the H1 experiment causes a reduction in rainfall over the Indian Ocean and Indian sub-continent (Figs 2 and 3) and thus heavier  $\delta^{18}\text{O}$  of precipitation over northern India. Further recycling of this isotopically heavy precipitation over the continents and subsequent transport into southern and eastern China causes the vapour that condenses and falls over China to also be isotopically heavier in the H1 than the LGM experiment (Supplementary Fig. S7). As in the observations, the simulated changes in  $\delta^{18}\text{O}_p$  in northern India are greater than those over eastern China (Fig. 2) because India also experiences changes in the seasonality of precipitation whereas China does not.

Finally, cooling of the Indian Ocean surface associated with the H1 event causes the evaporated water to be isotopically lighter than in the LGM simulation. This effect is small, however, compared with enrichment due to reduced precipitation over the Indian Ocean. Hence, water vapour exiting the Indian Ocean basin is, in the net, isotopically heavier in the H1 experiment.

### Indian Ocean SST responsible for $\delta^{18}\text{O}_p$ changes in China

To further illuminate the linkages between changes in climate and changes in isotopic composition of precipitation, we carried out three sensitivity experiments with the atmospheric model. Starting from the prescribed boundary conditions from the LGM experiment, we made regional modifications to the SST and sea-ice extent derived from the H1 experiment. These experiments were designed to isolate the impact of SST and sea-ice changes in the Atlantic (H1onlyATL experiment) and Indian Oceans (H1onlyIND and H1exceptIND experiments) on global temperature, precipitation and isotopic composition of precipitation (see Supplementary Information).

We find that changes in Indian Ocean SST alone (H1onlyIND) account for virtually all the decrease in precipitation over the Indian Ocean and subcontinent, and thus for the heavier  $\delta^{18}\text{O}_p$  over southern and eastern Asia seen in the H1 experiment (compare with Figs 2a and 3). The H1onlyATL experiment shows that the increase in North Atlantic sea-ice extent accounts for all the cooling at mid-to-high latitudes of the Northern Hemisphere (Supplementary Fig. S6) as well as colder, drier air being brought into the northern Indian Ocean basin, cooling the ocean surface as seen in the H1 experiment. In turn, the cooling of the northern Indian Ocean (H1 and H1onlyIND), which is most pronounced in winter but extends throughout the summer (Supplementary Fig. S8), causes a delayed onset and weakening of the Indian summer monsoon (ISM, Supplementary Fig. S9) and a weakening of convection over the Indian Ocean. Thus, the sudden increase in North Atlantic sea-ice extent in the H1 experiment impacts Indian Ocean climate and causes a sudden increase in  $\delta^{18}\text{O}_p$  over the Indian subcontinent, as well as isotopically heavier water vapour exported eastward into Southeast Asia.

In summary, our results illuminate the mechanism by which Heinrich events are recorded in the numerous proxy records throughout Asia. A large sudden increase in North Atlantic sea-ice extent causes a large decrease in temperature throughout a significant portion of the Northern Hemisphere, including the northern Indian Ocean, delaying the onset of the Indian monsoon and reducing monsoonal precipitation over the northern Indian Ocean and subcontinent. These climate changes cause precipitation over northern India to be reduced and isotopically heavier. As a consequence, vapour transported from the northern Indian basin into China—both directly and indirectly through recycling over the India subcontinent—has a heavier  $\delta^{18}\text{O}$  composition. Hence, the isotopic records of eastern Chinese caves are indicators of

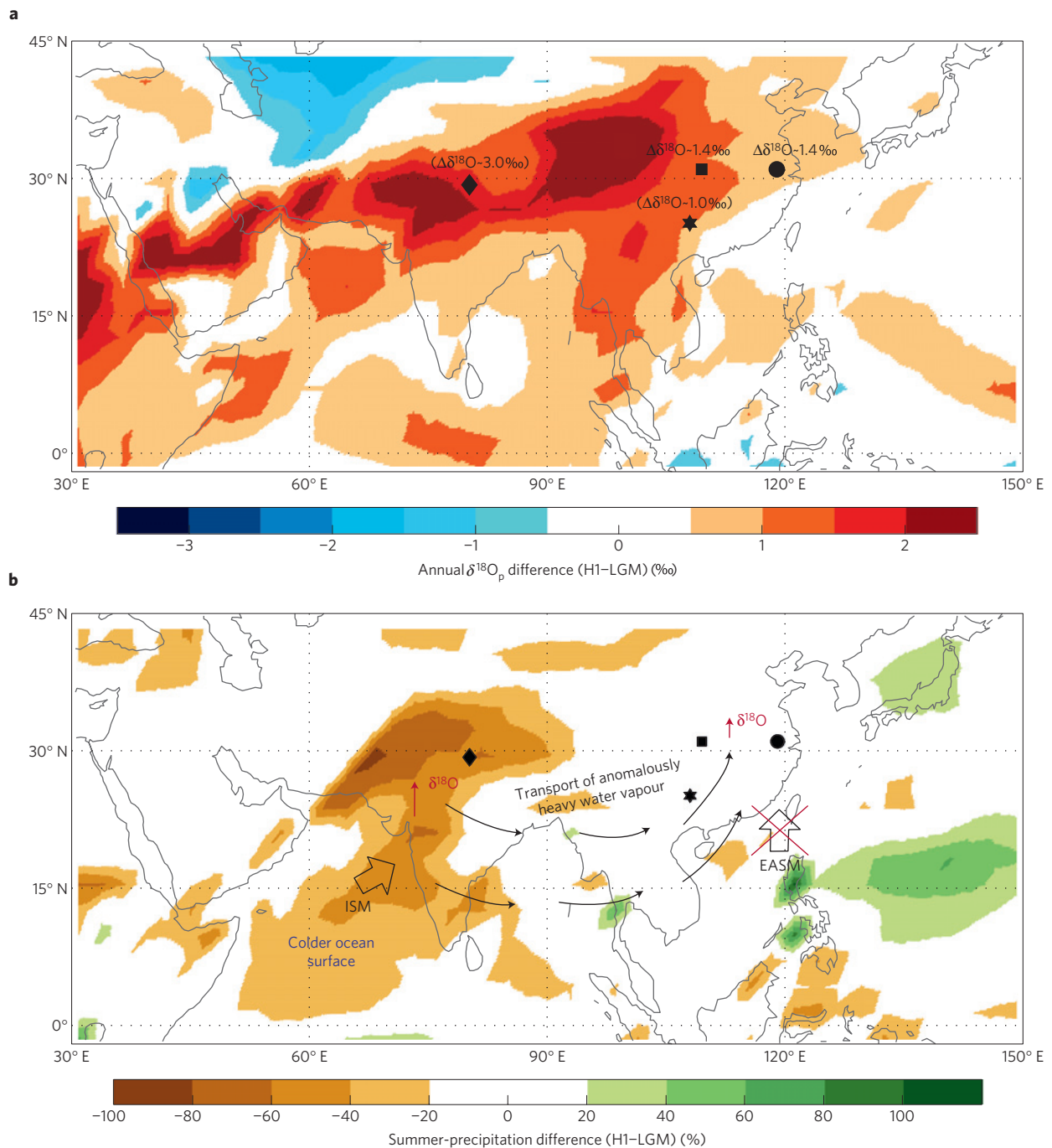


**Figure 2** |  $\delta^{18}\text{O}_p$  and summer precipitation difference between the H1 and LGM simulations. **a**, Changes in  $\delta^{18}\text{O}_p$  (Vienna Standard Mean Ocean Water, in ‰). **b**, changes in MJJA precipitation (%). Changes are plotted only when total MJJA precipitation exceeded 50 mm in the LGM simulation. Numbers in **a** indicate the observed change in  $\delta^{18}\text{O}_c$  (VPDB—Vienna Pee Dee Belemnite) during H1 (YD) at Hulu (circle), Songjia (square), Dongge (star) and Timta (diamond) caves. In addition, **b** shows a schematic representation of the mechanisms involved in the transfer of the  $\delta^{18}\text{O}$  signal from the Indian Ocean to eastern Chinese caves.

1 remote changes in the Indian basin associated with H-events: they  
2 are proxies for ISM rather than East Asian summer monsoon as  
3 previously thought<sup>11,13</sup>.

4 That the Chinese caves are recording non-local changes in the  
5  $\delta^{18}\text{O}$  of precipitation is in agreement with analyses of instrumental  
6 records across China<sup>19–21,31</sup> as well as previous model studies of  
7  $\delta^{18}\text{O}_p$  changes in the Holocene<sup>23</sup>. This result is also consistent  
8 with records of magnetic susceptibility in loess<sup>32</sup>, which indicate  
9 that there is little, if any, change in precipitation during the  
10 East Asian summer monsoon associated with H1. That abrupt

11 sea-ice changes in the North Atlantic cause abrupt changes in  
12 the strength of the ISM is supported by numerous proxy records  
13 and is evident for other H-events as well as Dansgaard–Oeschger  
14 events, which have recently been attributed to abrupt decreases in  
15 the North Atlantic sea-ice extent<sup>8,29</sup>. For example, proxy records  
16 from Greenland ice cores and sediment cores throughout the  
17 North Atlantic feature Dansgaard–Oeschger cycles that are tightly  
18 correlated with ocean-sediment records in the northwest Indian  
19 Ocean<sup>33,34</sup> and cave records in the Arabian Sea<sup>35</sup>, which have  
20 previously been interpreted as proxies for the strength of the ISM.

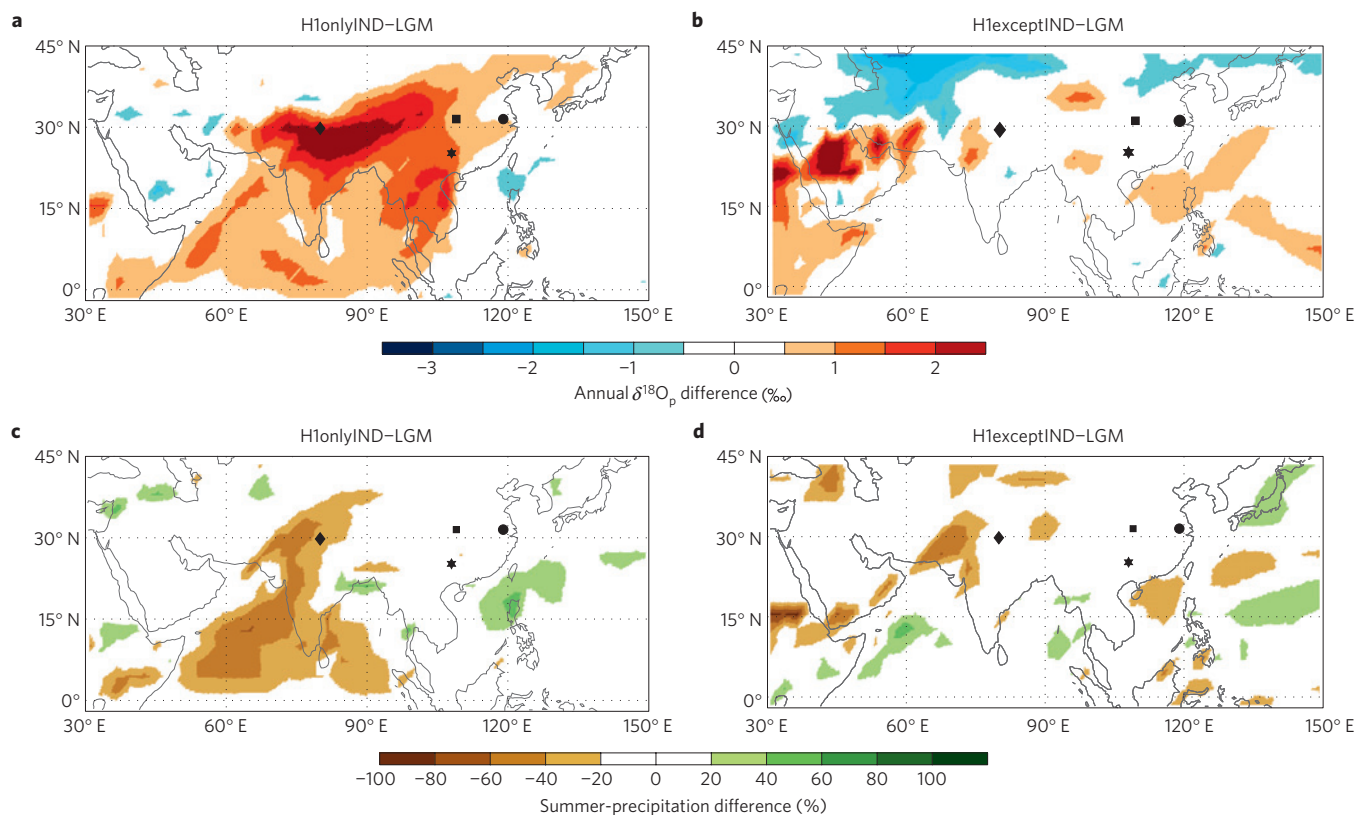


**Figure 3** |  $\delta^{18}\text{O}_p$  and summer-precipitation difference between the H1 sensitivity experiments and LGM simulation. **a–d**, Change with respect to LGM for the H1onlyIND (**a,c**) and H1exceptIND (**b,d**) experiments for  $\delta^{18}\text{O}_p$  Vienna Standard Mean Ocean Water (**a,b**, in ‰) and MJJA precipitation (**c,d**, in %). Changes are plotted only when total MJJA precipitation exceeds 50 mm in the LGM simulation. Markers indicate the locations of the following caves: Hulu (circle), Songjia (square), Dongge (star) and Timta (diamond).

1 Hence, the same processes that link expansion of sea ice in the North  
 2 Atlantic to an increase in  $\delta^{18}\text{O}_c$  in speleothems across China during  
 3 H-events are likely to be apropos to abrupt changes associated with  
 4 Dansgaard–Oeschger events (albeit with opposite sign).

5 Ref. 36 also examined the impact of a sudden freshwater pulse  
 6 into the North Atlantic on the climate and isotopic composition  
 7 of precipitation. That model did not simulate a significant change  
 8 in the ISM, nor did it reproduce the observed changes in  
 9  $\delta^{18}\text{O}_p$  in eastern China (for example, Hulu) and northern India  
 10 (for example, Timta) during an H-event. The authors attribute  
 11 the latter deficiencies to the coarse resolution of the model  
 12 ( $4^\circ \times 5^\circ$ ). Another important difference between that study and  
 13 ours, however, is the background climate state that is perturbed:  
 14 our freshwater pulse is applied to a simulated glacial period  
 15 (LGM) climate, whereas their pulse is applied to a modern-day  
 16 climate. Dynamical theory and GCM calculations demonstrate  
 17 that there are large differences in the response of the atmosphere  
 18 to forcing when ice sheets are present compared with modern-day  
 19 topography<sup>25,37</sup>. Furthermore, hosing experiments carried out  
 20 with the same climate model (CCSM3) show that the change in  
 21 precipitation over southern and eastern Asia due to hosing during  
 22 the Holocene is very different from that during the last glacial period  
 23 (Supplementary Fig. S10).

#### 24 Insights for understanding orbital variability 25 in speleothems

26 Finally, our results suggest a plausible explanation for the longer-  
 27 term (orbital) variability in  $\delta^{18}\text{O}_p$  in speleothems throughout  
 28 China, which is highly correlated with summer insolation in the  
 29 Northern Hemisphere subtropics. Modern ideas for the dynamics  
 30 of the monsoon suggest that the strength and duration of the

monsoon in the Indian Ocean and Southeast of Asia should  
 vary directly with changes in amplitude of the seasonal cycle  
 in the meridional gradient in SST in the deep tropics and  
 subtropics<sup>38,39</sup>, whereas the annual cycle of precipitation farther  
 north over China will be under the influence of a larger-scale  
 equator-to-pole gradient in insolation<sup>40</sup>. Orbitaly induced changes  
 in insolation force large precessional variations in the meridional  
 gradient of insolation in the tropics and hence should cause  
 large precessional variations in the strength and duration of  
 the Indian as well as South Asian (that is, to the south of  
 China) monsoons. On the basis of results from the present  
 study, previous modelling results<sup>23,36</sup> and analyses of modern-day  
 instrumental records of  $\delta^{18}\text{O}$  and precipitation over China<sup>21</sup>, we  
 propose that the large-amplitude precessional scale variability in  
 the  $\delta^{18}\text{O}_c$  in speleothems throughout China is due to precessional  
 forced changes in the strength of the Indian monsoon and  
 monsoon rainfall south of China that are in phase. Specifically,  
 we propose that precessional forcing causes in-phase variations  
 in the intensity of convection in the northern Indian Ocean and  
 over the ocean just south of China, and hence in-phase changes  
 in the efficiency of isotopic fractionation associated with deep  
 convection in these regions. As a consequence, there are in-phase  
 variations in the isotopic composition of vapour that originates  
 from these two monsoon regions and is subsequently advected  
 northward towards China and preserved in the speleothem records  
 across southern and eastern China. That dynamics internal to  
 the climate system can create changes in the Indian monsoon  
 that are of amplitude comparable to that associated with large  
 orbital forcing makes us reconsider what the climate system may  
 be capable of doing in response to more modest forcing, such as  
 increasing greenhouse gases.

## 1 Methods

2 The LGM experiment is a 440 year integration of the National Center for  
3 Atmospheric Research CCSM3 that was forced by boundary conditions at the  
4 LGM, approximately 21 kyr BP, including insolation, carbon dioxide concentration,  
5 the orography associated with the great ice sheets and a land configuration that  
6 reflects the lower LGM sea level<sup>24</sup>. Three further experiments with the CCSM3 that  
7 branched off this LGM simulation were carried out in ref. 25. In these experiments,  
8 16 Sv-yr volume of freshwater is instantly added to the upper 970 m of the North  
9 Atlantic and Arctic Oceans, causing a drop in salinity of 2 psu in these regions. The  
10 initial conditions for these experiments were taken from three different times in the  
11 LGM simulation (years 280, 340 and 400). For the LGM climate, we take the average  
12 of the last 100 years of the LGM CCSM3 simulation; for the H1 climate, we take the  
13 ensemble average for the decade following the freshwater dump.

14 The CCSM3 does not contain a module to simulate oxygen isotopes. Hence,  
15 for our study we use an uncoupled atmosphere global climate model, CAM3,  
16 with embedded stable water-isotope tracers<sup>28</sup> to simulate changes in the  $\delta^{18}\text{O}$  of  
17 precipitation during an archetypal abrupt climate change. We also tag ten different  
18 regions (Supplementary Fig. S4) to assess the origin of the water vapour that is  
19 transported to South and East Asia. This approach was used in ref. 41 to ascertain  
20 the origin of the water vapour of the precipitation falling over the Antarctic. The  
21 CAM3 atmospheric model is identical to the atmosphere model that is used in the  
22 coupled CCSM3 model.

23 We carried out two 15-year-long simulations with the CAM3 model. In each  
24 case we forced the model with the identical insolation, carbon dioxide, orography  
25 and boundary conditions that were used in the coupled (CCSM3) LGM and H1  
26 experiments. The uncoupled CAM3 LGM experiment uses the climatological SST  
27 and sea-ice extent from the CCSM3 LGM experiment, whereas the uncoupled  
28 CAM3 H1 experiment uses the ensemble-averaged SST and sea ice extent from  
29 the water-hosing experiments that were carried out using the CCSM3. Further  
30 sensitivity experiments were carried out with the uncoupled CAM3 model to isolate  
31 the relative importance of SST and sea-ice changes in various ocean basins to the  
32 simulated global climate and isotopic changes; these are described in more details  
33 in the Supplementary Information.

34 The isotopic composition of a sample is traditionally reported as the difference  
35 between the ratio of  $^{18}\text{O}$  to  $^{16}\text{O}$  measured in the sample (for example, calcite,  
36 precipitation and so on) and that measured in a standard (for example, for calcite  
37 the standard is the VPDB), and is defined as

$$\delta^{18}\text{O} = \left[ \frac{\frac{^{18}\text{O}_{\text{sample}}}{^{16}\text{O}_{\text{sample}}}}{\frac{^{18}\text{O}_{\text{standard}}}{^{16}\text{O}_{\text{standard}}}} - 1 \right] \times 10^3 \quad (1)$$

39 The oxygen isotopic composition of the stalagmite calcite ( $\delta^{18}\text{O}_{\text{c}}$ ) reflects the  
40 temperature of the cave and the  $\delta^{18}\text{O}$  of precipitation at the cave site which slowly  
41 percolates through the soil and is cemented in the geological record of speleothems.  
42 The temperature-dependent fractionation between calcite and water is of the order  
43 of  $-0.24\text{‰} \text{ } ^\circ\text{C}^{-1}$  (ref. 30) and the temperature in caves records the climatological  
44 mean annual surface temperature; however, variations in the  $\delta^{18}\text{O}$  of precipitation  
45 are generally much larger than those caused by temperature changes. As a result,  
46  $\delta^{18}\text{O}_{\text{c}}$  is thought to be a record of the precipitation-weighted  $\delta^{18}\text{O}$  ( $\delta^{18}\text{O}_{\text{p}}$ ):

$$\delta^{18}\text{O}_{\text{p}} = \frac{\sum(p\delta^{18}\text{O})}{\sum p} \quad (2)$$

48 where  $p$  and  $\delta^{18}\text{O}$  are the monthly averaged precipitation and isotopic composition  
49 of the precipitation, respectively, and the sum is over many years.

50 To assess the statistical significance of the differences in  $\delta^{18}\text{O}_{\text{p}}$  in the LGM  
51 and H1 experiments, we carry out a  $t$ -test. The  $\delta^{18}\text{O}_{\text{p}}$  in the H1 experiment is  
52 significantly different from that in the LGM experiment at the 5% confidence level  
53 over all South and East Asia.

54 Finally, we compared the simulated  $\delta^{18}\text{O}_{\text{p}}$  changes (H1 minus LGM) with  
55 the measured values associated with the H1-event for Hulu and Songjia caves and  
56 with that associated with the YD abrupt cooling event for Dongge and Timta caves,  
57 because the isotopic records at latter sites do not span the H1 event. The YD could  
58 be seen as an archetypal H-event, because it is characterized by a large freshwater  
59 discharge into the North Atlantic. In fact, YD is sometimes referred to as H0. We  
60 note that ref. 36 tabulates the isotopic changes in these and several further caves  
61 that are most probably associated with earlier H-events. The  $\delta^{18}\text{O}_{\text{p}}$  jumps seen in  
62 these earlier H-events are of similar amplitude and portray a similar spatial pattern  
63 to that simulated by our model.

64 Received 20 December 2010; accepted 4 May 2011;  
65 published online XX Month XXXX

## 66 References

- 67 1. Hemming, S. R. Heinrich events: Massive late Pleistocene detritus layers  
68 of the North Atlantic and their global climate imprint. *Rev. Geophys.* **42**,  
69 RG1005 (2004).
- 70 2. Heinrich, H. Origin and consequences of cyclic ice rafting in the Northeast  
71 Atlantic Ocean during the past 130,000 years. *Quat. Res.* **29**, 142–152 (1988).

3. Bond, G. *et al.* Evidence for massive discharges of icebergs into the North  
Atlantic Ocean during the last glacial period. *Nature* **360**, 245–249 (1992).
4. Overpeck, J., Anderson, D., Trumbore, S., Warren, P. & Prell, W. The southwest  
Indian monsoon over the last 18000 years. *Clim. Dyn.* **12**, 213–224 (1996).
5. Ganopolski, A. & Rahmstorf, S. Rapid changes of glacial climate simulated in a  
coupled climate model. *Nature* **409**, 153–158 (2001).
6. Chiang, J. C. H., Biasutti, M. & Battisti, D. S. Sensitivity of the Atlantic  
Intertropical Convergence Zone to Last Glacial Maximum boundary  
conditions. *Paleoceanography* **18**, 1094 (2003).
7. Jin, L., Chen, F., Ganopolski, A. & Claussen, M. Response of East Asian  
climate to Dansgaard/Oeschger and Heinrich events in a coupled model of  
intermediate complexity. *J. Geophys. Res.-Atmos.* **112**, D06117 (2007).
8. Li, C., Battisti, D. S. & Bitz, C. M. Can North Atlantic sea ice anomalies account  
for Dansgaard–Oeschger climate signals? *J. Clim.* **23**, 5457–5475 (2004).
9. Wang, Y. J. *et al.* Millennial- and orbital-scale changes in the East Asian  
monsoon over the past 224,000 years. *Nature* **451**, 1090–1093 (2008).
10. Zhou, H. *et al.* Distinct climate change synchronous with Heinrich event one,  
recorded by stable oxygen and carbon isotopic compositions in stalagmites  
from China. *Quat. Res.* **69**, 306–315 (2008).
11. Yuan, D. X. *et al.* Timing, duration, and transitions of the Last Interglacial  
Asian Monsoon. *Science* **304**, 575–578 (2004).
12. Sinha, A. *et al.* Variability of Southwest Indian summer monsoon precipitation  
during the Bølling–Allerød. *Geology* **33**, 813–818 (2005).
13. Wang, Y. J. *et al.* A high-resolution absolute-dated Late Pleistocene monsoon  
record from Hulu Cave, China. *Science* **294**, 2345–2348 (2001).
14. Cheng, H. *et al.* A penultimate glacial monsoon record from Hulu Cave and  
two-phase glacial terminations. *Geology* **34**, 217–220 (2006).
15. Cheng, H. Ice age terminations. *Science* **326**, 248–252 (2009).
16. Dansgaard, W. Stable isotopes in precipitation. *Tellus* **16**, 436–468 (1964).
17. Breitenbach, S. F. M. *et al.* Strong influence of water vapor source dynamics  
on stable isotopes in precipitation observed in Southern Meghalaya, NE India.  
*Earth Planet. Sci. Lett.* **292**, 212–220 (2010).
18. Cai, Y. *et al.* High-resolution absolute-dated Indian Monsoon record between  
53 and 36 ka from Xiaobailong Cave, southwestern China. *Geology* **34**,  
621–624 (2009).
19. Kelly, M. J. *et al.* High resolution characterization of the Asian Monsoon  
between 146,000 and 99,000 years B.P. from Dongge Cave, China and global  
correlation of events surrounding Termination II. *Palaeogeogr. Palaeoclimatol.*  
*Palaeoecol.* **236**, 20–38 (2006).
20. Johnson, K. R., Ingram, B. L., Sharp, W. D. & Zhang, P. Z. East Asian summer  
monsoon variability during Marine Isotope Stage 5 based on speleothem delta  
O-18 records from Wanxiang Cave, central China. *Palaeogr. Palaeoclimatol.*  
*Palaeoecol.* **236**, 5–19 (2006).
21. Dayem, K. E., Molnar, P., Battisti, D. S. & Roe, G. H. Lessons learned  
from oxygen isotopes in modern precipitation applied to interpretation of  
speleothem records of paleoclimate from eastern Asia. *Earth Planet. Sci. Lett.*  
**295**, 219–230 (2010).
22. Rozanski, K., Araguas-Araguas, L. & Gonfiantini, R. Isotopic patterns in  
modern global precipitation. Climate Change in Continental Isotopic Records.  
(ed Swart *et al.*) (AGU monograph, 1993).
23. LeGrande, A. N. & Schmidt, G. A. Sources of Holocene variability of oxygen  
isotopes in paleoclimate archives. *Clim. Past* **5**, 441–455 (2009).
24. Otto-Bliesner, B. L. *et al.* Last Glacial Maximum and Holocene climate in  
CCSM3. *J. Clim.* **19**, 2526–2544 (2009).
25. Bitz, C. M., Chiang, J. C. H., Cheng, W. & Barsugli, J. J. Rates of thermohaline  
recovery from freshwater pulses in modern, Last Glacial Maximum, and  
greenhouse warming climates. *Geophys. Res. Lett.* **34**, L07708 (2007).
26. Skinner, L. C. Revisiting the absolute calibration of the Greenland ice-core  
age-scales. *Clim. Past* **4**, 295–302 (2008).
27. Collins, *et al.* The formulation and atmospheric simulation of the Community  
Atmosphere Model version 3 (CAM3). *J. Clim.* **19**, 2144–2161 (2006).
28. Noone, D. & Sturm, C. *Isoscapes: Understanding Movement, Pattern, and Process  
on Earth Through Isotope Mapping* (Springer, 2009).
29. Li, C., Battisti, D. S., Schrag, D. P. & Tziperman, E. Abrupt climate shifts in  
Greenland due to displacements of the sea ice edge. *Geophys. Res. Lett.* **32**,  
L19702 (2005).
30. Friedman, I. & O'Neil, J. R. *Data of Geochemistry*. 6th edn (ed Fleischer, M.)  
(Geol. Surv. Prof. Pap. U.S., 1977).
31. Ding, Y. & Chan, J. C. L. The East Asian summer monsoon: An overview.  
*Meteorol. Atmos. Phys.* **89**, 117–142 (2005).
32. Sun, Y., An, Z., Clemens, S. C., Bloemendal, J. & Vandenberghe, J. Seven  
million years of wind and precipitation variability on the Chinese Loess Plateau.  
*Earth Planet. Sci. Lett.* **297**, 525–535 (2010).
33. Schulz, H., von Rad, U. & Erlenkeuser, H. Correlation between Arabian Sea  
and Greenland climate oscillations of the past 110,000 years. *Nature* **393**,  
54–57 (1998).
34. Altabet, M. A., Higgs, M. J. & Murray, D. W. The effect of millennial-scale  
changes in Arabian Sea denitrification on atmospheric CO<sub>2</sub>. *Nature* **415**,  
159–162 (2002).

- 1 35. Burns, S. J., Fleitmann, D., Matter, A., Kramers, J. & Al-Subbary, A. A.  
2 Indian Ocean climate and an absolute chronology over Dansgaard/Oeschger  
3 events 9 to 13. *Science* **301**, 1365–1367 (2003).
- 4 36. Lewis, S. C., LeGrande, A. N., Kelley, M. & Schmidt, G. A. Water vapour source  
5 impacts on oxygen isotope variability in tropical precipitation. *Clim. Past* **6**,  
6 325–343 (2010).
- 7 37. Swingedouw, D., Mignot, J., Braconnot, P., Mosquet, E. & Kageyama, M.  
8 Impact of freshwater release in the North Atlantic under different climate  
9 conditions in an OAGCM. *J. Clim.* **22**, 6377–6403 (2009).
- 10 38. Bordoni, S. & Schneider, T. Regime transitions of steady and time-dependent  
11 Hadley circulations: Comparison of axisymmetric and eddy-permitting  
12 simulations. *J. Atmosph. Sci.* **67**, 1643–1654 (2010).
- 13 39. Boos, W. R. & Kuang, Z. Dominant control of the South Asian monsoon by  
14 orographic insulation versus plateau heating. *Nature* **463**, 218–223 (2010).
- 15 40. Molnar, P., Boos, W. R. & Battisti, D. S. Orographic controls on climate and  
16 paleoclimate of Asia: Thermal and mechanical roles for the tibetan plateau.  
17 *Annu. Rev. Earth Planet. Sci.* **38**, 77–102 (2010).
- 18 41. Noone, D. & Simmonds, I. Annular variations in moisture transport  
19 mechanisms and the abundance of delta O-18 in Antarctic snow. *J. Geophys.*  
20 *Res.-Atmos.* **107**, 4742 (2002).

## Acknowledgements

This work is part of the ARCTREC and DecCen projects, funded by the Norwegian Research Council. D.S.B. was supported by the NSF EAR program (0908558). The authors would like to thank D. Noone for providing the isotope module for CAM3 and J. Bader and M. d.S. Mesquita for discussions and suggestions. This is publication no A323 from the Bjerknes Centre for Climate Research.

## Author contributions

F.S.R.P. and D.S.B. conceived the study, analysed the results and wrote the manuscript. F.S.R.P. designed and carried out the experiments, and processed the model results. K.H.N. analysed the results and edited the manuscript. C.M.B. wrote the tagging code in the isotope module and set up CAM3 to run in LGM with isotopes and tagging.

## Additional information

The authors declare no competing financial interests. Supplementary information accompanies this paper on [www.nature.com/naturegeoscience](http://www.nature.com/naturegeoscience). Reprints and permissions information is available online at <http://www.nature.com/reprints>. Correspondence and requests for materials should be addressed to F.S.R.P.

## Page 1

---

*Query 1: Line no. 1*

Please note that the first paragraph has been edited according to style.

*Query 2: Line no. 20*

Please clarify ‘ the precipitation-weighted  $\delta^{18}\text{O}$  of precipitation’.

*Query 3: Line no. 31*

Please provide postcode for all affiliations.

## Page 2

---

*Query 4: Line no. 1*

‘blue’ changed to ‘white’ in fig. 1 caption to match fig.—is this correct? If not, please clarify.

*Query 5: Line no. 4*

According to style, line headings should not exceed one line in length; please provide a shorter heading that will fit in one line.

## Page 5

---

*Query 6: Line no. 16*

Please give GCM in full.

## Page 6

---

*Query 7: Line no. 37*

Equations (1) and (2) are not cited in text. As per journal style numbered equations should be cited in the text. If they are not cited, equation numbers that are not cited will be deleted from the equations and the remaining equations will be renumbered. OK?

*Query 8: Line no. 80*

Please provide page range for ref. 6.